



Nicotine and its metabolite cotinine target MD2 and inhibit TLR4 signaling

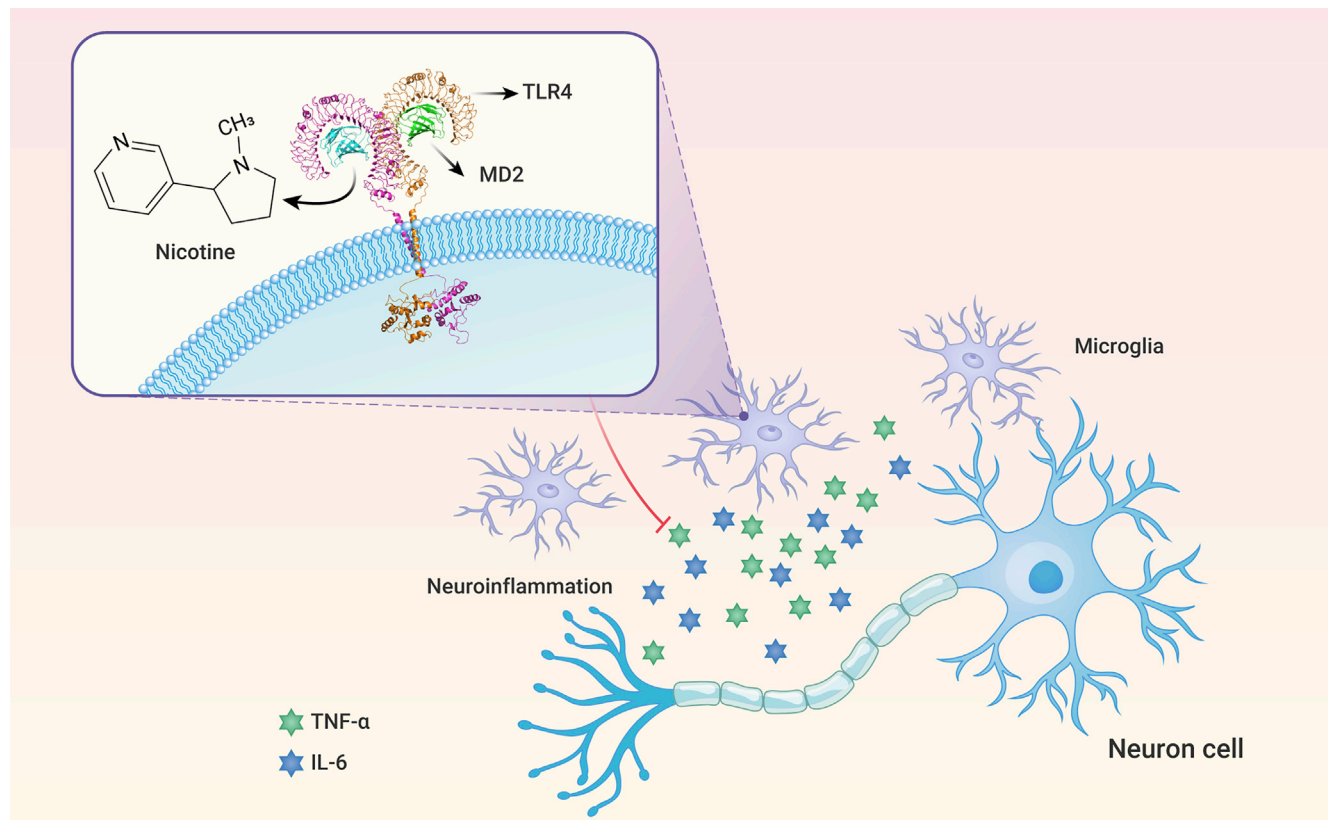
Hongyuan Li,^{1,7} Yinghua Peng,^{2,7} Cong Lin,¹ Xiaozheng Zhang,¹ Tianshu Zhang,¹ Yibo Wang,¹ Yuanpeng Li,¹ Siru Wu,¹ Hongshuang Wang,¹ Mark R. Hutchinson,^{3,6} Linda R. Watkins,⁴ and Xiaohui Wang^{1,5,*}

*Correspondence: xiaohui.wang@ciac.ac.cn

Received: September 26, 2020; Accepted: April 27, 2021; Published Online: April 29, 2021; <https://doi.org/10.1016/j.xinn.2021.100111>

© 2021 The Author(s). This is an open access article under the CC BY-NC-ND license (<http://creativecommons.org/licenses/by-nc-nd/4.0/>).

Graphical abstract



Public summary

- Nicotine and cotinine bind to MD2 in microglia cell
- Nicotine and cotinine inhibit the expression of pro-inflammatory factors
- The activity of nicotine and cotinine in microglia is independent of nAChRs



Nicotine and its metabolite cotinine target MD2 and inhibit TLR4 signaling

Hongyuan Li,^{1,7} Yinghua Peng,^{2,7} Cong Lin,¹ Xiaozheng Zhang,¹ Tianshu Zhang,¹ Yibo Wang,¹ Yuanpeng Li,¹ Siru Wu,¹ Hongshuang Wang,¹ Mark R. Hutchinson,^{3,6} Linda R. Watkins,⁴ and Xiaohui Wang^{1,5,*}

¹Laboratory of Chemical Biology, Changchun Institute of Applied Chemistry, Chinese Academy of Sciences, Jilin 130022, China

²Institute of Special Animal and Plant Sciences, Chinese Academy of Agricultural Sciences, Jilin 130112, China

³Discipline of Physiology, Adelaide Medical School, University of Adelaide, Adelaide, SA, Australia

⁴Department of Psychology and Neuroscience, and the Center for Neuroscience, University of Colorado at Boulder, Boulder, CO 80309, USA

⁵Department of Applied Chemistry and Engineering, University of Science and Technology of China, Hefei 230026, China

⁶ARC Centre of Excellence for Nanoscale Biophotonics, University of Adelaide, Adelaide, SA 5000, Australia

⁷These authors contributed equally

*Correspondence: xiaohui.wang@ciac.ac.cn

Received: September 26, 2020; Accepted: April 27, 2021; Published Online: April 29, 2021; <https://doi.org/10.1016/j.xinn.2021.100111>

© 2021 The Author(s). This is an open access article under the CC BY-NC-ND license (<http://creativecommons.org/licenses/by-nc-nd/4.0/>).

Citation: Li H., Peng Y., Lin C., et al., (2021). Nicotine and its metabolite cotinine target MD2 and inhibit TLR4 signaling. *The Innovation* 2(2), 100111.

Nicotine is the principal alkaloid of tobacco often manufactured into cigarettes and belongs to a highly addictive class of drugs. Nicotine attenuates the neuroinflammation induced by microglial activation. However, the molecular target(s) underlying anti-inflammatory action of nicotine has not been fully understood. Considering the psychoactive substances morphine, cocaine, and methamphetamine act as xenobiotic-associated molecular patterns and can be specifically sensed by the innate immune receptor Toll-like receptor 4 (TLR4), here we sought to delineate whether nicotine and/or its metabolite cotinine may be recognized by the innate immune system via myeloid differentiation protein 2 (MD2), an accessory protein of TLR4 that is responsible for ligand recognition. MD2-intrinsic fluorescence titrations, surface plasmon resonance, and competitive displacement binding assays with curcumin (MD2 probe) demonstrated that both nicotine and cotinine targeted the lipopolysaccharide (LPS; TLR4 agonist) binding pocket of MD2 with similar affinities. The cellular thermal shift assay indicated that nicotine binding increased, while cotinine binding decreased, MD2 stability. These biophysical binding results were further supported by *in silico* simulations. In keeping with targeting MD2, both nicotine and cotinine inhibited LPS-induced production of nitric oxide and tumor necrosis factor alpha (TNF- α) and blocked microglial activation. Neither a pan nicotinic acetylcholine receptor (nAChR) inhibitor nor RNAi for nAChRs abolished the suppressive effect of nicotine- and cotinine-induced neuroinflammation. These data indicate that TLR4 inhibition by nicotine and cotinine at the concentrations tested in BV-2 cells is independent of classic neuronal nAChRs and validate that MD2 is a direct target of nicotine and cotinine in the inhibition of innate immunity.

Keywords: nicotine; cotinine; Toll-like receptor 4; myeloid differentiation protein 2; microglia; molecular dynamics simulation

INTRODUCTION

Toll-like receptor 4 (TLR 4) is a conserved innate immune receptor.¹ Together with the accessory protein myeloid differentiation protein 2 (MD2), TLR4 detects pathogen-associated molecular patterns (PAMPs), damage-associated molecular patterns (DAMPs), and xenobiotic-associated molecular patterns (XAMPs).²

Nicotine is the principal alkaloid of tobacco that is most closely linked to the addictive properties of smoking.³ Nicotine attenuates neuroinflammation induced by microglial activation in the central nervous system (CNS), an action assumed to arise via classic nicotinic acetylcholine receptors (nAChRs).^{4,5} The $\alpha 7$ nAChR-microRNA-124 signaling axis^{6,7} has been reported to mediate the cholinergic anti-inflammatory effect. However, the molecular target(s) underlying the anti-inflammatory actions of nicotine are

not fully understood. Considering the recent studies that the psychoactive xenobiotics morphine,⁸ cocaine,⁹ and methamphetamine¹⁰ can be specifically sensed by TLR4/MD2, we sought to delineate whether nicotine and/or its metabolite cotinine may be recognized by the innate immune system via TLR4/MD2. The results of biophysical binding, *in silico* simulations, and cellular characterizations consistently showed that MD2 is a direct target of nicotine and cotinine.

RESULTS

Nicotine and cotinine bind to MD2

MD2, a co-receptor of TLR4, is responsible for ligand recognition.¹¹ Fluorescence quenching titration of MD2 was first performed to explore innate immune recognition of nicotine and cotinine by TLR4. As shown in Figure 1A, nicotine and cotinine binding each caused quenching of MD2-intrinsic fluorescence. By fitting the titration curves with a one-site binding model, dissociation constants (K_D) of 12.3 ± 1.0 and 13.5 ± 1.0 μ M were obtained for nicotine and cotinine interacting with MD2, respectively. As a comparison, roxithromycin, a compound used as a negative control in MD2 binding,¹² showed negligible MD2 fluorescence quenching, demonstrating the specific binding of nicotine and cotinine to MD2. Figure 1B presents the $\log(F_0/F-1)$ versus $\log([\text{ligand}]/\mu\text{M})$ plots. A stoichiometry of 1.18 ± 0.03 and a K_D of 11.0 ± 1.6 μ M were obtained for the binding of nicotine to MD2; a stoichiometry of 1.12 ± 0.02 and a K_D of 13.4 ± 1.8 μ M were obtained for cotinine binding to MD2. These results justify the one-site binding model used for the nonlinear least-square fit of the MD2 quenching data (Figure 1A). Protein A was used as negative control protein and no apparent quenching of protein A-intrinsic fluorescence was observed when titrating with nicotine/cotinine (Figure S1), indicating that the interaction of MD2 with nicotine and cotinine are specific. To further confirm the recognition of nicotine and cotinine by MD2, surface plasmon resonance (SPR) was performed. Nicotine (Figure 1C) and cotinine (Figure 1D) interacted with MD2 with the K_D values of 23.1 ± 1.2 and 14.1 ± 1.8 μ M, respectively. The binding affinities determined by SPR were slightly different from those derived from the protein-intrinsic fluorescence quenching assays. This is not surprising considering that the underlying principles of these two methods are different.

Fluorescence probe curcumin binds to the lipopolysaccharide (LPS) binding pocket of MD2, and its fluorescence intensity enhances when binding to MD2.¹³ As shown in Figure S2, nicotine and cotinine caused a concentration-dependent decrease of curcumin fluorescence from the curcumin-MD2 complex, suggesting that nicotine/cotinine replaces curcumin binding in the LPS binding pocket of MD2. In contrast, the negative control compound roxithromycin induced negligible decrease in curcumin fluorescence, again supporting that nicotine and cotinine specifically interact with MD2.

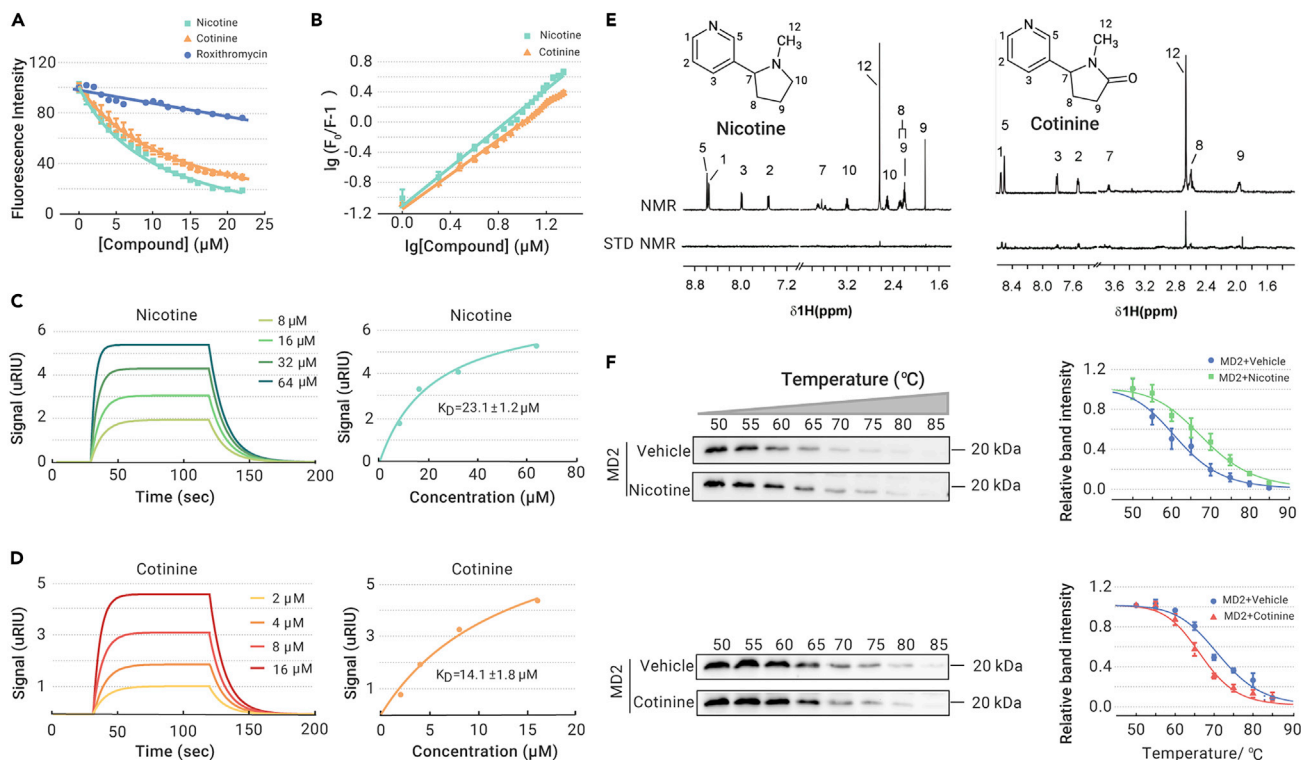


Figure 1. Biophysical characterizations of nicotine and cotinine binding with MD2 (A) Titration curves of MD2-intrinsic fluorescence with increasing compound concentration. Excitation at 280 nm and emission at 337 nm (peak position) was plotted against the titrated compound concentration. K_d values of 12.3 ± 1.0 and 13.5 ± 1.0 μM were derived by nonlinear least-squares fit of a one-site binding model for interacting with MD2. Roxithromycin, which has been shown to have no apparent binding affinity to MD2, was used as the negative control compound. (B) The binding curves shown in (A) were plotted according to the equation: $\lg(F_0/F-1)$ versus $\lg([\text{compound}]/\mu\text{M})$. $K_d = 11.0 \pm 1.6$ μM and $n = 1.18 \pm 0.03$ were derived for nicotine binding to MD2; $K_d = 13.4 \pm 1.8$ μM and $n = 1.12 \pm 0.02$ were derived for cotinine binding to MD2. (C and D) SPR analysis of nicotine (C) and cotinine (D) binding to the MD2 protein. (E) STD-NMR of nicotine/cotinine (400 μM) with MD2 (4 μM). ^1H NMR assignments of nicotine and cotinine are also given. (F) Cellular thermal shift assay of MD2 with nicotine and cotinine. Nicotine binding increases MD2 thermal stability ($\Delta T_m = 6.5^\circ\text{C} \pm 1.6^\circ\text{C}$), while cotinine decreases MD2 stability ($\Delta T_m = -4.2^\circ\text{C} \pm 0.5^\circ\text{C}$). All experiments were performed three times independently, and data are given as the mean \pm SEM.

Saturation transfer difference NMR (STD-NMR) spectroscopy allows the detection of transient (fast) binding of small-molecule ligands to macromolecule receptors and is a powerful tool for investigating the mild to weak ligand-protein interaction ($K_d > \sim 10^{-5}$ M).¹⁴ This was used to explore the molecular recognition of MD2 with nicotine and cotinine. STD-NMR directly measures NMR signals from the ligand itself and shows only those protons from the ligand that interact by saturation transfer from the protein, thus identifying the chemical moieties of the ligand involved in binding.¹⁵ The STD-NMR spectrum obtained for the complex of MD2 with both nicotine and cotinine and the reference spectra of nicotine and cotinine are shown in Figure 1E. Strong STD signals from cotinine were readily observable, which supports that cotinine is an active ligand of MD2. However, no STD signals were observed for nicotine, which disagrees with results from the MD2-intrinsic fluorescence quenching titration and curcumin competitive displacement binding assays that nicotine specifically interacts with MD2.

It should be noted that STD-NMR requires that the ligand-protein complex is in fast exchange on the NMR timescale and relies on the rapid exchange between the bound and free states.¹⁶ Although nicotine and cotinine bind to MD2 with similar affinities, which are close to the upper limit of the ligand-protein interaction ($K_d = 10$ μM) suitable for STD-NMR measurement, most likely they behave differently on the MD2 conformation. It is quite possible that nicotine binding stabilizes the MD2 conformation, which decreases the exchange rate of nicotine between the bound and the free states, therefore leading to a false negative of STD-NMR.

To directly investigate the effects of nicotine and cotinine on MD2 conformation stability and explore whether MD2 could be an endogenous target of nicotine and cotinine in the cellular context, cellular thermal shift assay (CETSA) was performed. CETSA is based on the discovery that protein melting curves can be generated and that drug binding leads to very

significant shift of its melting temperature (T_m).¹⁷ The purified MD2 protein is very stable ($T_m \sim 80^\circ\text{C}$).⁸ CETSA of purified MD2 protein showed nicotine binding increased MD2 protein stability, whereas cotinine binding decreased MD2 stability (Figure S3). Similar results were obtained for CETSA of endogenous MD2 in cell lysate (Figure 1F). Nicotine increased the T_m value of MD2 by $6.5^\circ\text{C} \pm 1.6^\circ\text{C}$ (Figure 1F), which supports the speculation derived from STD-NMR that nicotine binding stabilizes the MD2 conformation. In contrast to nicotine, cotinine decreased MD2 stability ($\Delta T_m = -4.2^\circ\text{C} \pm 0.5^\circ\text{C}$) (Figure 1F), which indicates that cotinine binding increases the MD2 conformation flexibility. Compared with nicotine, cotinine would be in faster exchange between the bound and free states. Therefore, the STD-NMR spectrum of the complex of MD2 and cotinine was observed while no STD signals were measured for the nicotine-MD2 complex. Although nicotine and cotinine behaved differently on the MD2 stability, CETSA data show that they directly bind to MD2 in a cellular context. In all, these biophysical binding data suggest that MD2 is a direct target of nicotine and cotinine.

Molecular recognition of nicotine and cotinine by MD2

To investigate how nicotine and cotinine interact with MD2, computational simulations were performed. The best docking poses with lowest energy of nicotine and cotinine interacting with MD2 are given in Figure 2A and 2B, respectively. Nicotine and cotinine were both found to dock into the conserved hydrophobic cavity of MD2 and overlap with the R3' chains of lipid A, which is consistent with the curcumin competitive displacement binding assay result that nicotine and cotinine bind to the LPS binding pocket of MD2. The best docking poses were refined using MD simulations. The root-mean-square deviation (RMSD) values of MD2 (Figure S4) reached stability during 100 ns of MD simulations. Protein flexibility revealed by RMSD showed that the conformation of the MD2 bound to cotinine was more

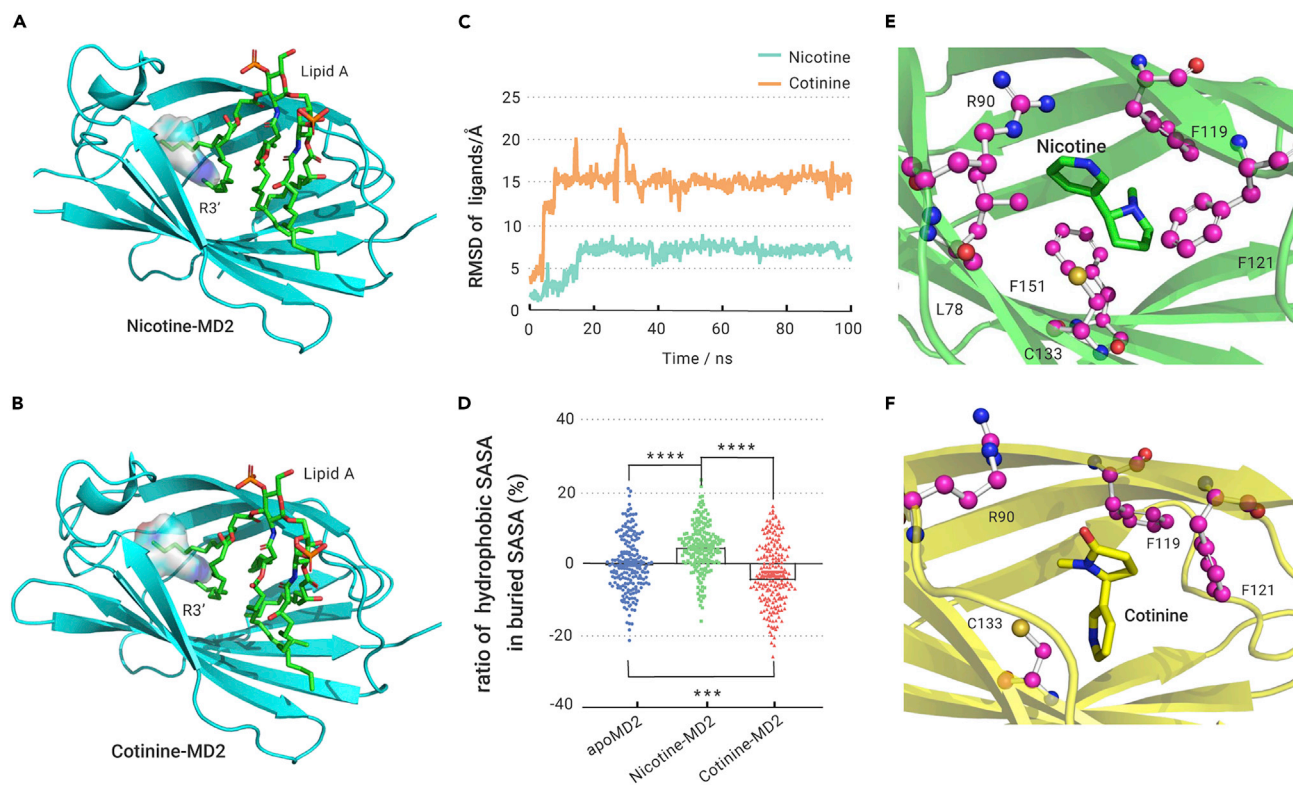


Figure 2. *In silico* simulation of nicotine and cotinine interacting with MD2 (A and B) Overlap of the best docking pose of nicotine (A) and cotinine (B) with lipid A. Nicotine and cotinine occupied the LPS binding location (acyl chains R3'). MD2 is shown as cyan cartoon; lipid A is shown as a green stick model; nicotine and cotinine are shown as a cyan surface model. (C) Time evolution of the RMSD of nicotine (black) and cotinine (red) during the MD simulations at 310.15 K. (D) The changes of the ratio of the hydrophobic SASA in the buried SASA of MD2 upon binding to nicotine and cotinine. Data were calculated based on the last 20 ns equilibrated MD trajectories at 310.15 K. *** $p < 0.001$, **** $p < 0.0001$. (E and F) The calculated binding mode of nicotine (E) and cotinine (F) with MD2 at 310.15 K. The ligand is shown as a stick model. MD2 is shown as a cartoon. Key residues of MD2 in interacting with ligands are shown as a ball and stick model.

flexible than that of MD2 interacted with nicotine, which is agreement with results of the STD-NMR and CETSA. The RMSD of the ligands during MD simulations was also monitored (Figure 2C). Cotinine had much higher RMSD values than nicotine. This result shows that cotinine is more flexible than nicotine in the ligand-MD2 complex. Compared with nicotine, cotinine would have a faster exchange between the free form and the MD2 bound state, which supports the speculation derived from the STD-NMR experiment.

The detailed binding mode of nicotine and cotinine with MD2 was subsequently investigated. Figure 2D shows the representative pose of nicotine binding to MD2 during the molecular dynamic simulations. The heterocycles of nicotine were surrounded by hydrophobic residues L78, F119, F121, and F151 of MD2. The nitrogen of the pyridine moiety from nicotine interacted with R90 and C133 of MD2 through polar interactions. Cotinine interacted with F199 and F121 of MD2 by hydrophobic interactions, and the oxygen of the carbonyl moiety formed polar interactions R90 and C133 (Figure 2E). The binding free energies calculated using the MM-PBSA method showed that nicotine (-12.2 ± 0.2 kcal/mol) and cotinine (-11.3 ± 0.1 kcal/mol) had similar MD2 binding free energies, which is consistent with the biophysical measurements of the K_D values.

Solvent-accessible surface areas (SASA) were calculated to further investigate the ligand binding-induced conformational changes of MD2. The SASA of MD2 did not change upon binding with nicotine or cotinine (Figure S5A). Both the buried SASA (Figure S5B) and the exposed SASA (Figure S5C) did not change upon interacting with nicotine or cotinine. Interestingly, further analysis showed that nicotine binding increased the percentage of hydrophobic area in the buried SASA of MD2, while cotinine decreased the ratio of hydrophobic area in the buried SASA (Figure 2F). It should be noted that the hydrophobic residues prefer to be buried inside owing the hydrophobic interactions, therefore increasing the folding and stability of the protein.¹⁸ These *in silico* simulation results explicitly explain

that nicotine binding increases MD2 stability while cotinine decreases MD2 stability.

Nicotine and cotinine inhibition of LPS-induced pro-inflammatory factors in microglia BV-2 cells is independent of nAChRs

Microglia are CNS immunocompetent cells and are key mediators of neuroinflammation.¹⁹ To investigate the actions of nicotine and cotinine on neuroinflammation, the effects of nicotine and cotinine on LPS-induced signaling and the downstream pro-inflammatory factors were measured in the BV-2 microglial cell line, which reproduces many of the responses of primary microglia with high fidelity.²⁰ Nicotine and cotinine inhibited the LPS-induced MyD88 recruitment to TLR4 and suppressed the formation of the TLR4/MD2/MyD88 complex (Figures 3A and 3B). LPS stimulation significantly increased the phosphorylation of IRAK1, IRAK4, IKK β , p65, and p38. Both nicotine (Figures 3C and 3D) and cotinine (Figures 3E and 3F) significantly inhibited the LPS-induced phosphorylation of these TLR4 signaling factors.

The effects of nicotine and cotinine on the LPS-induced downstream pro-inflammatory factors were next investigated. Nicotine (Figure 4A) and cotinine (Figure 4B) inhibited LPS-induced nitric oxide (NO) overproduction in a concentration-dependent manner with half-maximal inhibitory concentration values of 0.8 ± 0.1 and 0.5 ± 0.1 mM, respectively, which were in agreement with previous reports that high concentrations (>1 mM) of nicotine were needed for *in vitro* microglial cellular assays.²¹ Cell viability was also tested by crystal violet staining assay, and no apparent cellular toxicities of nicotine (Figure 4A) or cotinine (Figure 4B) were observed, even at a concentration of 1.6 mM. This eliminates the possibility of the observed inhibition of LPS-induced pro-inflammatory factors by nicotine and cotinine being due to cell death.

In addition to NO, the pro-inflammatory cytokines interleukin-6 (IL-6), Cyclooxygenase-2 (COX-2), and tumor necrosis factor alpha (TNF- α) were also

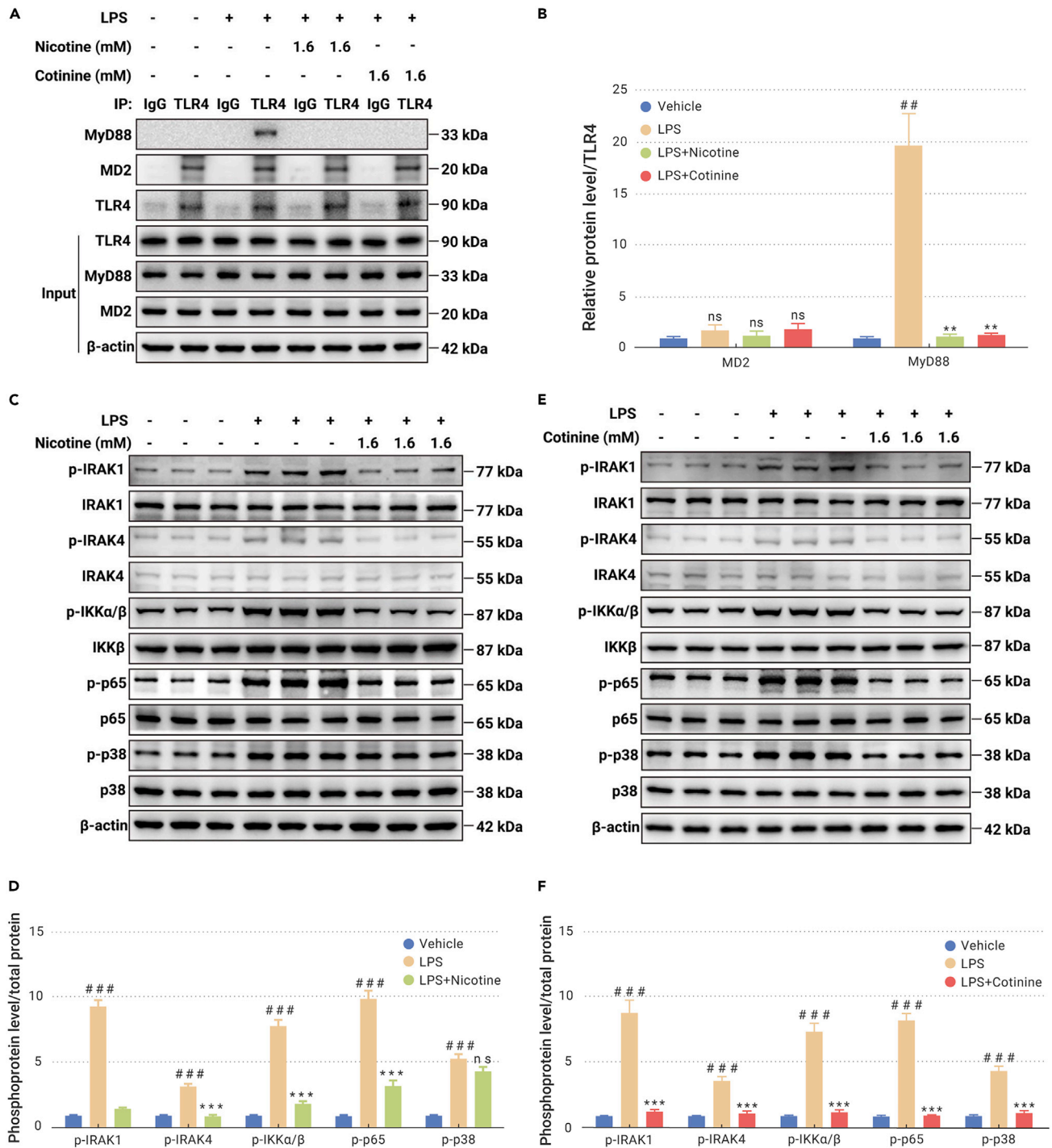


Figure 3. Cellular characterizations of nicotine and cotinine on TLR4 signaling BV-2 cells were administered 200 ng/mL LPS and the indicated concentration of nicotine or cotinine for 1 h. (A and B) The co-immunoprecipitation of anti-TLR4 antibody. MD2, TLR4, and MyD88 were detected by western blotting. (C–F) The effect of nicotine (C and D) and cotinine (E and F) on the LPS-induced phosphorylation of IRAK1, IRAK4, IKKβ, p65, and p38. All experiments were performed three times independently, and data are given as the mean ± SEM. ###p < 0.001 versus the control; ***p < 0.01 versus the LPS group; ns, not significant versus the LPS group.

measured by qRT-PCR. LPS stimulation significantly increased mRNA expression of IL-6 (Figures 4C and 4D), COX-2 (Figures 4E and 4F), and TNF-α (Figures 4G and 4H) relative to the control in 24 h, especially at the 6-h time point. Generally, nicotine and cotinine inhibited LPS-induced IL-6, COX-2, and TNF-α. Nicotine and cotinine inhibited LPS-induced TNF-α mRNA (Figures 4G and 4H) and protein (Figure S6) with similar kinetic patterns. However, the kinetic profiles of nicotine and cotinine in inhibiting LPS-induced IL-6 and COX-2 were different. At the 2-h time point, only IL-6 mRNA

was inhibited by cotinine at concentrations of 0.8 and 1.6 mM. At the 6-h time point, both 1.6 mM nicotine and cotinine suppressed LPS-induced IL-6 and COX-2 mRNAs. At the 24-h time point, cotinine inhibited LPS-induced IL-6 and COX-2 mRNA expression in a concentration-dependent manner. However, nicotine (0.8 and 1.6 mM) failed to inhibit LPS-induced IL-6 and COX-2 mRNAs and the corresponding proteins (Figure S7) at the 24-h time point. The expressions of IL-6, COX-2, and TNF-α cytokines are not only controlled by the transcription factor nuclear factor κB (NF-κB). Several

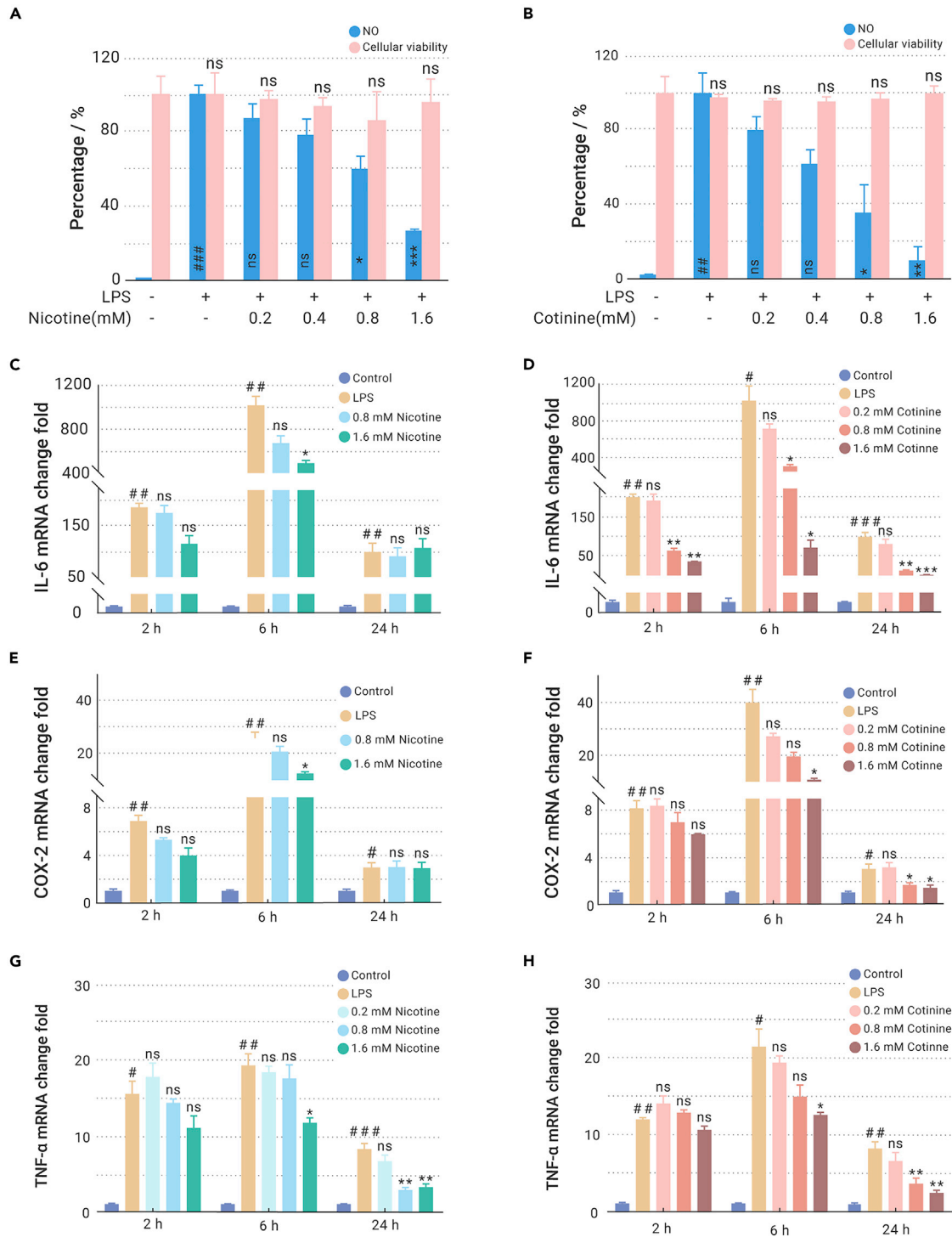


Figure 4. The effect of nicotine and cotinine on the LPS-induced downstream pro-inflammatory factors BV-2 cells were administered 200 ng/mL LPS and the indicated concentration of nicotine (A, C, E, and G) or cotinine (B, D, F, and H). Cellular viability and the pro-inflammatory factors NO (A and B), IL-6 mRNA (C and D), COX-2 mRNA (E and F), and TNF- α mRNA (G and H) were measured at three different time points in 24 h. All experiments were performed three to four times independently, and data are given as the mean \pm SEM. # p < 0.05 versus the control; ## p < 0.01 versus the control; ### p < 0.001 versus the control; * p < 0.05 versus the LPS group; ** p < 0.01 versus the LPS group; *** p < 0.001 versus the LPS group; ns, not significant versus the LPS group.

other factors are also involved in the regulating these genes (Figure S8). It is not surprising that the compounds inhibiting NF- κ B do not necessarily inhibit the downstream cytokines with the similar kinetic patterns. In addition to pro-inflammatory factors, increased ROS and phagocytosis are also hallmarks of microglial activation. As shown in Figure S9, LPS stimulation increased H₂O₂ (Figure S9A) and the phagocytic activity (Figure S9B) of

BV-2 cells. These were inhibited by nicotine and cotinine in a concentration-dependent manner. Together, these data show that nicotine and cotinine inhibit microglial activation as reflected by suppression of both LPS-induced pro-inflammatory factor overproduction and microglial phagocytosis.

Nicotine and cotinine are classic agonists of nAChRs,²² among which α 7 nAChR and α 4 β 2 nAChR are the evolutionarily oldest nAChRs and

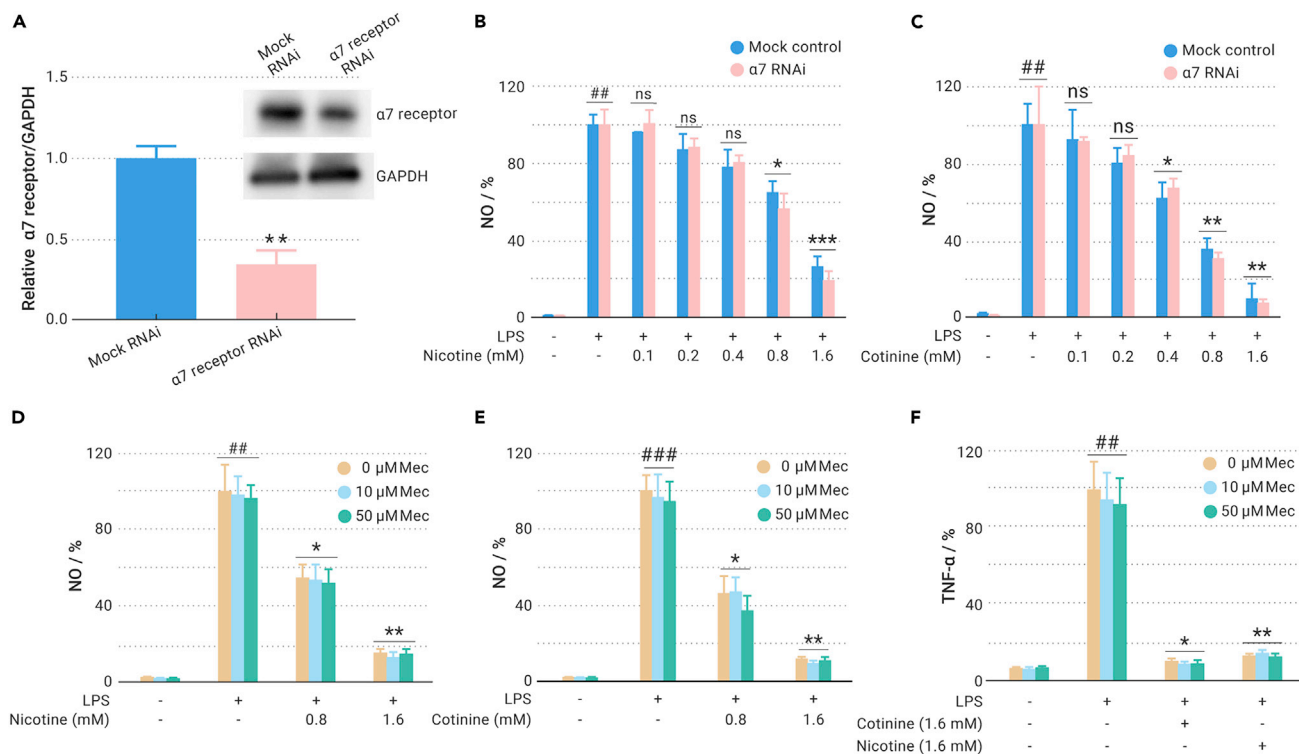


Figure 5. Blockage of nAChRs by RNAi or chemical agent does not attenuate nicotine and cotinine inhibiting LPS-induced pro-inflammatory factors (A) Western blotting analysis of $\alpha 7$ nicotinic receptor in a stable $\alpha 7$ RNAi cell line and mock RNAi cells. (B and C) The effect of nicotine (B) and cotinine (C) on the LPS-induced NO production in $\alpha 7$ nicotinic receptor knockdown cells. (D and E) The effect of nonselective nAChR antagonist mecamylamine (Mec) on nicotine (D) and cotinine (E) blocking LPS-induced NO overproduction. (F), the effect of Mec on nicotine and cotinine blocking LPS-induced TNF- α protein overproduction. Cells were treated with LPS (200 ng/mL) and the indicated concentrations of nicotine/cotinine. After treatment for 24 h, supernatants were collected for NO assay and TNF- α ELISA. $n = 3-4$ independent experiments, and data are given as the mean \pm SEM. ## $p < 0.01$ versus the control; ### $p < 0.001$ versus the control; * $p < 0.05$ versus the LPS group; ** $p < 0.01$ versus the LPS group; *** $p < 0.01$ versus the LPS group; ns, not significant versus the LPS group.

predominate in CNS.²³ RNAi was performed to determine whether either $\alpha 7$ nAChR or $\alpha 4\beta 2$ nAChR are involved in inhibition of LPS-induced pro-inflammatory factors in microglial BV-2 cells by either nicotine or cotinine. Stable $\alpha 7$, $\alpha 4$, and $\beta 2$ subunits of nAChR knocking down cell lines were constructed by lentivirus transduction and puromycin selection. Western blot analysis showed that $\alpha 7$ nAChR (Figure 5A), as well as $\alpha 4$ and $\beta 2$ subunits (Figure S10A), were knocked down by $\sim 70\%$ – 90% by RNAi compared with the mock control. $\alpha 7$ nAChR knockdown did not block either nicotine (Figure 5B) or cotinine (Figure 5C) inhibition of LPS-induced NO. Knockdown of $\alpha 4$ and $\beta 2$ subunits also failed to affect nicotine and cotinine inhibition of LPS-induced NO (Figure S10B). To substantiate the results from the RNAi, mecamylamine (Mec), which is an nAChR antagonist with non-selectivity toward individual isotypes,²⁴ was used to pharmacologically block nAChRs to define whether this would disrupt nicotine and cotinine actions in inhibiting LPS-induced pro-inflammatory factors. It should be noted that the typical working concentration of Mec is 10 μM .⁵ Neither 10 nor 50 μM Mec treatment attenuated nicotine (Figure 5D) or cotinine (Figure 5E) inhibition of LPS-induced NO in BV-2 cells. Mec also did not affect nicotine or cotinine inhibition of LPS-induced TNF- α (Figure 5F). These data indicate that TLR4 inhibition by nicotine and cotinine is independent of their well-known nAChR targets and support the notion that MD2 is a novel target of nicotine and cotinine in the inhibition of innate immunity.

DISCUSSION

Based on the innate immune recognition of TLR4 with psychoactive substances including morphine,⁸ cocaine,⁹ and methamphetamine,^{10,25} as well as other MD2 ligands,²⁶⁻³² XAMPs have been proposed as one type of TLR4 ligand, beyond the classic PAMPs and DAMPs.² Nicotine is the major addictive component of tobacco and belongs to a class of drugs that is second only to opioids in addiction liability.³³ Herein, we are interested in whether

nicotine and its main metabolite cotinine could be recognized by TLR4/MD2 as XAMPs. MD2-intrinsic fluorescence titrations, SPR, and curcumin competitive displacement binding assays showed that both nicotine and its metabolite cotinine targeted the LPS binding pocket of MD2 with similar affinities, which was further supported by binding mode analysis and MM-PBSA free energy calculations during MD simulations. CETSA found that nicotine binding increased the MD2 thermal stability while cotinine decreased the MD2 stability, which is consistent with MD2 RMSD analysis that nicotine binding stabilized the MD2 conformation and cotinine increased the flexibility of MD2. Compared with nicotine, cotinine was more flexible in the ligand-MD2 complex as revealed by ligand RMSD analysis, which agreed well with the speculation derived from the STD-NMR that cotinine would have a faster exchange between the free form and the MD2 bound state compared with nicotine. In agreement with the conclusion from CETSA, *in silico* simulations found that nicotine binding increased the percentage of hydrophobic areas in the buried SASA of MD2, while cotinine decreased the percentage of hydrophobic areas in the buried SASA, although the bindings of nicotine and cotinine showed no significant effect to the total SASA, the buried SASA, or the exposed SASA. These computational simulations rationalize the opposite behaviors of nicotine and cotinine on MD2 from the biophysical chemistry perspective. In keeping with targeting MD2, nicotine and cotinine inhibited induction of NO and TNF- α and blocked microglial phagocytosis by the TLR4 agonist LPS.

Nicotine is the principal alkaloid of tobacco,³⁴ and approximately 70%–80% of nicotine is converted to cotinine, which has a long half-life and does not have cardiovascular or addictive side effects.³⁵ Smoking a cigarette yields about 1–2 mg of absorbed nicotine, which is readily transported to the brain with the concentration of ~ 300 nM.³⁶ Nicotine interacts with nAChRs and acts as a cholinergic agonist with affinities of nM to low μM ,³⁵ while the affinity of cotinine for nAChRs is >100 -fold less potent than nicotine.³⁷ Also, there is a striking differential between the potencies

for the nicotine- and cotinine-induced behavioral responses as measured by the delayed-matching-to-sample task in animals, wherein cotinine is ~30- to 2,000-fold less effective than nicotine.³⁸ Here, nicotine and cotinine were found to be specifically recognized by TLR4 accessory protein MD2 with similar binding affinities, although they showed opposite effects on the MD2 protein stability and flexibility. In contrast to cotinine showing much less nAChR agonist activity than nicotine, cotinine was slightly more potent in inhibiting LPS-induced pro-inflammatory factors compared with nicotine in microglial BV-2 cells. Considering the contrasting behaviors of nicotine and cotinine toward nAChRs,^{37,38} it is unlikely that the classic nAChR-mediated cholinergic anti-inflammatory pathway was responsible for nicotine and cotinine inhibiting LPS-induced inflammation in BV-2 cells. Blocking nAChRs by RNAi ($\alpha 7$, $\alpha 4$, and $\beta 2$ subunits) and by the pan nAChR inhibitor Mec did not alter the suppressive effect of nicotine and cotinine, which supports the conclusion that nAChRs are unlikely to be the targets of nicotine and cotinine in suppressing the LPS-induced inflammation in microglial BV-2 cells.

In sum, this study provides direct evidence that the anti-neuroinflammatory effect of nicotine and cotinine is, at least in part, mediated by the inhibition of TLR4 signaling. Nicotine and cotinine target the LPS binding pocket of MD2, albeit behaving differently on MD2 stability. Nicotine and cotinine inhibit LPS-induced NO and TNF- α and block microglial activation as reflected by enhanced phagocytosis. Neither RNAi of nAChRs nor pan nAChR inhibition abolish either nicotine- or cotinine-induced suppressive effect of neuroinflammation. These data indicate that TLR4 inhibition by nicotine and cotinine at the concentrations tested in BV-2 cells is independent of classic nAChRs and validate that MD2 is a direct target of nicotine and cotinine in the inhibition of innate immunity. This work furthers our understanding of the mechanisms underlying the nicotine neuroimmunomodulation, which would be of paramount importance for its translational applications.

MATERIALS AND METHODS

Materials

Nicotine, cotinine, curcumin, roxithromycin, 2,3-diaminonaphthalene, anti-GAPDH primary antibody, and anti- β -actin antibody were purchased from Sigma-Aldrich (St. Louis, MO, USA). Ultrapure LPS and puromycin were obtained from InvivoGen (San Diego, CA, USA). The Vybrant Phagocytosis Assay Kit, the Quantitative Peroxide Assay Kit, RIPA buffer, protease inhibitor cocktails, and SuperSignal West Pico Chemiluminescent Substrate were purchased from Thermo Fisher Scientific (Waltham, MA, USA). The RNeasy Mini Kit, the RT2 Easy First Strand cDNA Synthesis Kit, PCR primers, and SYBR Green PCR Master Mix were obtained from QIAGEN (Frederick, MD, USA). Primary MD2 antibody, TLR4 antibody, anti- $\alpha 7$ nAChR antibody, anti- $\beta 2$ nAChR antibody, and anti- $\alpha 4$ nAChR antibody were purchased from Abcam (Cambridge, MA, USA). Anti-IL6 antibody was purchased from ImmunoWay (Plano, TX, USA); anti-IRAK1 antibody was purchased from Proteintech (Wuhan, Hubei, China); anti-Phospho-IRAK1 (Thr209) antibody, and anti-COX2 antibody were purchased from Abways Technology (Shanghai, China); anti-MyD88 antibody, anti-IRAK4 antibody, anti-Phospho-IRAK4 (Thr345/Ser346) antibody, anti-IKK β , anti-Phospho-IKK α/β (Ser176/180) antibody, anti-p38 MAPK antibody, anti-Phospho-p38 MAPK (Thr180/Tyr182) antibody, anti-NF- κ B p65 antibody, and anti-Phospho-NF- κ B p65 (Ser536) antibody were purchased from Cell Signaling Technology (Danvers, MA, USA). The TNF- α ELISA kit and the TMB substrate reagent set were purchased from BD Biosciences (San Jose, CA, USA). Well-characterized $\alpha 7$ nAChR ($\alpha 7$ nAChR) shRNA lentiviral transduction particles (TRCN0000102955), $\beta 2$ nAChR shRNA lentiviral transduction particles (TRCN0000103020), $\alpha 4$ nAChR shRNA lentiviral transduction particles (TRCN0000102860), and mock control transduction particles were obtained from the Functional Genomic Facility in the BioFrontiers Institute of the University of Colorado at Boulder under the license of Sigma-Aldrich (St. Louis, MO, USA).

Methods

More information is available in the [supplemental information file](#).

REFERENCES

- Takeuchi, O., and Akira, S. (2010). Pattern recognition receptors and inflammation. *Cell* **140**, 805–820.
- Wang, Y., Zhang, S., Li, H., et al. (2020). Small-molecule modulators of toll-like receptors. *Acc. Chem. Res.* **53**, 1046–1055.
- Li, H., Wang, K., Yao, J., et al. (2019). Research progress in the development of nicotine as a medicine. *Prog. Pharm. Sci.* **43**, 824–831.
- Park, H.J., Lee, P.H., Ahn, Y.W., et al. (2007). Neuroprotective effect of nicotine on dopaminergic neurons by anti-inflammatory action. *Eur. J. Neurosci.* **26**, 79–89.
- Lutz, J.A., Kulshrestha, M., Rogers, D.T., et al. (2014). A nicotinic receptor-mediated anti-inflammatory effect of the flavonoid rhamnetin in BV2 microglia. *Fitoterapia* **98**, 11–21.
- Sun, Y., Li, Q., Gui, H., et al. (2013). microRNA-124 mediates the cholinergic anti-inflammatory action through inhibiting the production of pro-inflammatory cytokines. *Cell Res.* **23**, 1270–1283.
- Qin, Z., Wan, J.J., Sun, Y., et al. (2017). Nicotine protects against DSS colitis through regulating microRNA-124 and STAT3. *J. Mol. Med. (Berl)* **95**, 221–233.
- Wang, X., Loram, L.C., Ramos, K., et al. (2012). Morphine activates neuroinflammation in a manner parallel to endotoxin. *Proc. Natl. Acad. Sci. U S A* **109**, 6325–6330.
- Northcutt, A.L., Hutchinson, M.R., Wang, X., et al. (2015). DAT isn't all that: cocaine reward and reinforcement require Toll-like receptor 4 signaling. *Mol. Psychiatry* **20**, 1525–1537.
- Zhang, X., Wang, Y., Wang, H., et al. (2020). Exploring methamphetamine nonenanti-selectively targeting Toll-like receptor 4/myeloid differentiation protein 2 by in silico simulations and wet-lab techniques. *J. Chem. Inf. Model.* **60**, 1607–1613.
- Rajamanickam, V., Yan, T., Xu, S.M., et al. (2020). Selective targeting of the TLR4 co-receptor, MD2, prevents colon cancer growth and lung metastasis. *Int. J. Biol. Sci.* **16**, 1288–1302.
- Resman, N., Gradisar, H., Vasl, J., et al. (2008). Taxanes inhibit human TLR4 signaling by binding to MD-2. *FEBS Lett.* **582**, 3929–3934.
- Gradisar, H., Keber, M.M., Pristovsek, P., et al. (2007). MD-2 as the target of curcumin in the inhibition of response to LPS. *J. Leukoc. Biol.* **82**, 968–974.
- Angulo, J., and Nieto, P.M. (2011). STD-NMR: application to transient interactions between biomolecules—a quantitative approach. *Eur. Biophys. J.* **40**, 1357–1369.
- Viegas, A., Manso, J., Nobrega, F.L., et al. (2011). Saturation-transfer difference (STD) NMR: a simple and fast method for ligand screening and characterization of protein binding. *J. Chem. Educ.* **88**, 990–994.
- Maity, S., Gundampati, R.K., and Kumar, T.K.S. (2019). NMR methods to characterize protein-ligand interactions. *Nat. Prod. Commun.* **14**, 1–17.
- Jafari, R., Almqvist, H., Axelsson, H., et al. (2014). The cellular thermal shift assay for evaluating drug target interactions in cells. *Nat. Protoc.* **9**, 2100–2122.
- Tych, K.M., Batchelor, M., Hoffmann, T., et al. (2016). Differential effects of hydrophobic core packing residues for thermodynamic and mechanical stability of a hyperthermophilic protein. *Langmuir* **32**, 7392–7402.
- Gray, S.C., Kinghorn, K.J., and Woodling, N.S. (2020). Shifting equilibria in Alzheimer's disease: the complex roles of microglia in neuroinflammation, neuronal survival and neurogenesis. *Neural Regen. Res.* **15**, 1208–1219.
- Henn, A., Lund, S., Hedtjarn, M., et al. (2009). The suitability of BV2 cells as alternative model system for primary microglia cultures or for animal experiments examining brain inflammation. *ALTEX* **26**, 83–94.
- Morioka, N., Hisaoka-Nakashima, K., and Nakata, Y. (2018). Regulation by nicotinic acetylcholine receptors of microglial glutamate transporters: role of microglia in neuroprotection. In *Nicotinic Acetylcholine Receptor Signaling in Neuroprotection*, pp. 73–88.
- Uriarte, I., Perez, C., Caballero-Mancebo, E., et al. (2017). Structural studies of nicotins: cotinine versus nicotine. *Chemistry* **23**, 7238–7244.
- Schuller, H.M. (2009). Is cancer triggered by altered signalling of nicotinic acetylcholine receptors? *Nat. Rev. Cancer* **9**, 195–205.
- Lippiello, P.M., Beaver, J.S., Gatto, G.J., et al. (2008). TC-5214 (S-(+)-mecamylamine): a neuronal nicotinic receptor modulator with antidepressant activity. *CNS Neurosci. Ther.* **14**, 266–277.
- Wang, X., Northcutt, A.L., Cochran, T.A., et al. (2019). Methamphetamine activates Toll-like receptor 4 to induce central immune signaling within the ventral tegmental area and contributes to extracellular dopamine increase in the nucleus accumbens shell. *ACS Chem. Neurosci.* **10**, 3622–3634.
- Peng, Y., Zhang, X., Zhang, T., et al. (2019). Lovastatin inhibits Toll-like receptor 4 signaling in microglia by targeting its co-receptor myeloid differentiation protein 2 and attenuates neuropathic pain. *Brain Behav. Immun.* **82**, 432–444.
- Zhang, X.Z., Peng, Y.H., Grace, P.M., et al. (2019). Stereochemistry and innate immune recognition: (+)-norbinaltorphimine targets myeloid differentiation protein 2 and inhibits Toll-like receptor 4 signaling. *FASEB J.* **33**, 9577–9587.
- Zhang, X.Z., Cui, F.C., Chen, H.Q., et al. (2018). Dissecting the innate immune recognition of opioid inactive isomer (+)-naltrexone derived Toll-like receptor 4 (TLR4) antagonists. *J. Chem. Inf. Model.* **58**, 816–825.
- Selfridge, B.R., Wang, X., Zhang, Y., et al. (2015). Structure-activity relationships of (+)-naltrexone-inspired Toll-like receptor 4 (TLR4) antagonists. *J. Med. Chem.* **58**, 5038–5052.
- Wang, X., Zhang, Y., Peng, Y., et al. (2016). Pharmacological characterization of the opioid inactive isomers (+)-naltrexone and (+)-naloxone as antagonists of Toll-like receptor 4. *Br. J. Pharmacol.* **173**, 856–869.
- Park, S.H., Kim, N.D., Jung, J.K., et al. (2012). Myeloid differentiation 2 as a therapeutic target of inflammatory disorders. *Pharmacol. Ther.* **133**, 291–298.

32. Zhang, X., Zhang, T., Cui, F., et al. (2016). Toll-like receptor 4 small molecule modulators. *Chin. J. Chem.* **33**, 876–886.
33. Hatsukami, D.K. (2018). Reducing nicotine in cigarettes to minimally addictive levels a new frontier for tobacco control. *JAMA Psychiatry* **75**, 987–988.
34. Crooks, P.A., and Dvoskin, L.P. (1997). Contribution of CNS nicotine metabolites to the neuropharmacological effects of nicotine and tobacco smoking. *Biochem. Pharmacol.* **54**, 743–753.
35. Matta, S.G., Balfour, D.J., Benowitz, N.L., et al. (2007). Guidelines on nicotine dose selection for in vivo research. *Psychopharmacology* **190**, 269–319.
36. Cuevas-Olguin, R., Esquivel-Rendon, E., Vargas-Mireles, J., et al. (2020). Nicotine smoking concentrations modulate GABAergic synaptic transmission in murine medial prefrontal cortex by activation of alpha7* and beta2* nicotinic receptors. *Eur. J. Neurosci.* **51**, 781–792.
37. Riah, O., Dousset, J.C., Courriere, P., et al. (1999). Evidence that nicotine acetylcholine receptors are not the main targets of cotinine toxicity. *Toxicol. Lett.* **109**, 21–29.
38. Buccafusco, J.J., and Terry, A.V. (2003). The potential role of cotinine in the cognitive and neuroprotective actions of nicotine. *Life Sci.* **72**, 2931–2942.

ACKNOWLEDGMENTS

This work was supported by the National Natural Science Foundation of China (91956121, 21877106, 21807098, and 21850410455), the Chinese Academy of Sciences (CAS) Pioneer Hundred Talents Program, the Young Talents Program of the Chinese Academy of Agricultural Sciences, and the Natural Science Foundation of Jilin Province (20180101021JC).

Computing time was supported by the Network and Computing Center, Changchun Institute of Applied Chemistry, CAS, the National Supercomputing Center in Guangzhou, and the National Supercomputing Center in Shenzhen. M.R.H. is the recipient of an ARC Future Fellowship (FT180100565) and Director of the Australian Research Council Centre of Excellence for Nanoscale BioPhotonics (CE140100003).

AUTHOR CONTRIBUTIONS

X.W. designed the research. H.L., Y.P., C.L., X.Z., T.Z., Y.L., and S.W. performed the research. H.L., Y.P., Y.W., H.W., and X.W. analyzed the data. M.R.H., L.R.W., and X.W. wrote the paper.

DECLARATION OF INTERESTS

The authors declare that they have no conflict of interest.

SUPPLEMENTAL INFORMATION

Supplemental information can be found online at <https://doi.org/10.1016/j.xinn.2021.100111>.

LEAD CONTACT WEBSITE

<http://medchem.ciac.jl.cn/>